Effect of state of charge on Type IV hydrogen storage tank rupture in a fire

Kashkarov, S.[1], Molkov, V.[2] and Makarov, D.[3]
[1] Hydrogen Safety Engineering and Research Centre (HySAFER), Ulster University, Newtownabbey, BT37 0QB, UK, s.kashkarov@ulster.ac.uk
[2] v.molkov@ulster.ac.uk
[3] dv.makarov@ulster.ac.uk

ABSTRACT

The use of hydrogen storage tanks at 100% of nominal working pressure NWP is expected only after refuelling. Driving between refuellings is characterised by the state of charge SoC<100%. There is experimental evidence that Type IV tanks tested in a fire at initial pressures below one-third of its NWP, depending on a fire source, were leaking without rupture. This paper aims at understanding this phenomenon and the development of a predictive model. The numerical research has demonstrated that the heat transfer from fire through the composite overwrap is sufficient to melt the polymer liner. This initiates hydrogen microleaks through the composite wall before it loses the load-bearing ability when the resin degrades deep enough to cause the tank to rupture. The dependence of tank fire-resistance rating (FRR) on the SoC is presented for tanks of volume in the range 36-244 L. The tank wall thickness non-uniformity, i.e. thinner composite at the dome area, is identified as a serious issue for tank's fire resistance that must be addressed by tank manufacturers and OEMs. The effect of the burst pressure ratio on FRR is investigated. It is concluded that thermal parameters of the composite wall, i.e. decomposition heat and temperatures, play a vital role in simulations of tank failure and thus FRR.

NOMENCLATURE

c_p	specific heat capacity	J/kg/K
D	diameter	m
H_d	resin heat of decomposition	J/kg
L	length	m
m	mass	kg
P	pressure	Pa
$q"$	heat flux	W/m^2
S	thickness	m
T	temperature	K
V	tank volume	m^3
λ	thermal conductivity	W/m/K
ρ	density	kg/m^3

Subscripts

$b.min.$	burst minimum pressure
$CFRP$	carbon fibre reinforced polymer
d	decomposition
ext	external
$HDPE$	high-density polyethylene
$H2$	hydrogen
$load\ b.$	load-bearing
NWP	nominal working pressure
$TPRD$	thermally activated pressure relief device

Abbreviations

BPR	Burst pressure ratio
CFRP	Carbon fibre reinforced polymer
CHSS	Compressed hydrogen storage system
FRR	Fire-resistance rating

GTR	Global Technical Regulation
HDPE	High-density polyethylene
NWP	Nominal working pressure
RCS	Regulations, codes and standards
SAE	Society of Automotive Engineers
SoC	State of charge
TPRD	Thermally activated pressure relief device

1.0 INTRODUCTION

It was demonstrated previously that the risk of using hydrogen vehicles on London roads is acceptable if the tank's fire-resistance rating (FRR), i.e. time from fire initiation to tank rupture is above 50 min [1]. This was concluded considering the a thermally activated pressure relief device (TPRD) is not activated in localised fire or blocked from the fire in the accident. The assessment was performed for scenarios of an onboard hydrogen storage tank filled to 100% of nominal working pressure (NWP). The pressure of the compressed hydrogen storage system (CHSS) is not always at NWP, i.e. the state of charge (SoC) is below 100%. SAE J2601 defines the SoC as the "ratio of CHSS hydrogen density to the density at NWP rated at the standard temperature 15ºC": SoC=[ρ(P, T)/ρ(NWP, 15 ºC)]×100 [2]. The use of hydrogen tank capacity at NWP (SoC=100%) is characteristic for a period immediately after tank refuelling only. Fig. 1 shows the tank SoCs calculated for different temperatures (20°C, 30°C and 85°C, the latter is the regulated temperature limit for fuelling [2],[3]).

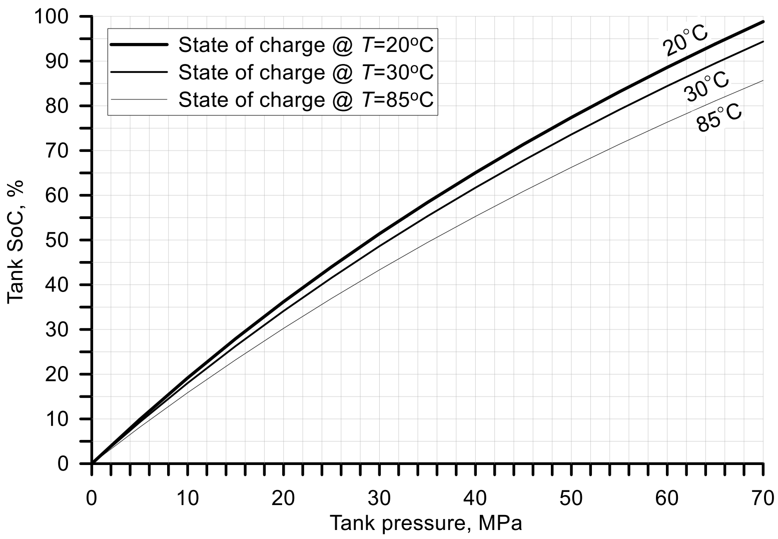

Figure 1. Tank SoC as a function of storage pressure at temperatures 20ºC, 30ºC and 85ºC.

In the experimental work [4] NWP=70 MPa Type IV tanks of 36 L were tested in localised and engulfing fires without TRPD at different SoC to define their FRR (initial pressures were 70.3, 70.6, 35.6 and 17.8 MPa). The fire source was a heptane pan of an area of 0.96 m^2. Tanks filled at 70.3 MPa and 70.6 MPa ruptured after 6 min 32 s and 5 min 20 s respectively. The first fire test was engulfing fire and the second tank was tested in localised ("partial") fire. The first important conclusion from these experiments was that the time to tank rupture did not depend on whether the tank was subject to engulfing or localised fire. The second conclusion was that the tank would not withstand the localised portion of the fire test which lasted 10 min following the GTR#13 protocol as the tank would rupture in less than 10 min in the heptane spill fire. The authors recommended that the "cylinder as a whole needs to be protected from localised fire impact" [4].

These experiments also demonstrated that when one of the NWP=70 MPa tanks was filled at 35.6 MPa (51% NWP) and underwent the same engulfing fire, it ruptured later – after 9 min 49 s (almost 1.5 times longer FRR compared to the first tank filled at practically NWP, i.e. at 70.3 MPa). This can be justified if the original composite tank failure in a fire mechanism [5] is applied. The mechanism states that when inward propagating resin decomposition front meets the outward "propagating" load-bearing fraction of the composite wall thickness, a tank ruptures. In this test with reduced initial pressure, the load-bearing thickness sufficient to withstand the internal pressure without rupture is smaller and thus longer time is required for the resin decomposition front to reach it.

Finally, in the experiments with the tank filled at lower pressure of 17.8 MPa (25% NWP) the leakage of hydrogen without tank rupture was observed at 11 min 4 s. In this case, the wall thickness fraction that was not load-bearing was large enough to allow for heat transfer to melt the liner while the remaining undamaged composite wall still was able to bear the reduced internal pressure load. The authors reported that hydrogen "was leaking across its entire surface with slightly more leakages at the ends" and that during the test "epoxy resin seems to have disappeared but the carbon fibres did not burn" [4].

There is another experimental study on fire testing of NWP=70 MPa 36 L Type IV tanks at different initial pressures [6]. There were no hydrogen gas temperature measurements, but the composite in-thickness integrated thermocouples were showing the initial temperatures of about 42ºC (315 K). The fire source was represented in this study by a hydrogen diffusion burner consisting of 4 pipes directed at tanks from two opposite sides. The filling pressures of the tanks were 70 MPa (NWP), 52.5 MPa (75% NWP), 25 MPa (36% NWP) and 10 MPa (14% NWP). The first two tanks, one at pressure 70 MPa and another at 52.5 MPa, ruptured after 3 min 58 s and 5 min 11 s respectively. The other two tanks filled at lower pressures, i.e. 25 MPa and 10 MPa respectively, did not rupture but leaked after 6 min 40 s and 8 min 10 s respectively. These experiments, even performed with a different fire source, have confirmed the conclusions of the previous study [4] that the lower initial pressures in the tank avail the larger portion of the composite wall thickness that is not load-bearing and thus can be thermally decomposed by heat flux from the fire without compromising the tank wall load-bearing ability and enabling longer time for the heat transfer to the liner sufficient to melt it and initiate release.

The UN Global technical regulation on hydrogen and fuel cell vehicles No.13 (GTR#13) [3], the EC No. 406/2010 implementing the Regulation No.79/2009 [7] establish the minimum burst pressure, $P_{b.min.}$, for tanks overwrapped with carbon fibre reinforced polymer (CFRP) as 2.25 times of NWP (burst pressure ratio). This means that for the NWP=70 MPa tank, its wall will be able to withstand up to 2.25x70 MPa=157.5 MPa. There are discussions at GTR#13 IWG SGS on the reduction of this burst pressure ratio from BPR=2.25 to BPR=2.00. It must be underlined that this is only the minimum requirement and any higher value is accepted especially if the safety not only availability of carbon fibre is at the stake, e.g. BPR=2.5 which is quite common. To the best of the authors' knowledge, the effect of the BPR on the FRR of tanks was not studied and published.

The original tank failure in a fire mechanism suggested at Ulster University has proved to work well in predicting the tank FRR. For the entire tank wall thickness S_{CFRP} withstanding 157.5 MPa only its fraction of 1/2.25=0.44 is sufficient to withstand NWP=70 MPa. The remainder of the fraction 1-0.44=0.56 would be called here as "load+" that can be decomposed by heat flux from fire without tank rupture (thus reducing burst pressure ratio to BPR=1). If the pressure inside the tank increases above 70 MPa, e.g. due to increasing temperature because of heat transfer from a fire, the load-bearing wall thickness fraction, $S_{load\ b.}$, increases proportionally and, thus, the "load+" fraction decreases. In the event of a fire, the higher is the pressure the thinner is the fraction "load+" and the faster it will degrade (for particular heat flux from a fire that correlates with specific heat release rate HRR/A) causing tank rupture. If the pressure inside the tank decreases, e.g. due to blowdown in a fire through TPRD, $S_{load\ b.}$ will decrease respectively, allowing for longer and more heat transfer inside the tank with subsequent liner melting, while resin decomposition front has more thickness in the increasing with blowdown time "load+" fraction of the wall to travel through. This is the mechanism behind "no rupture but a leak" of tanks in fire tests with lower compared to NWP initial hydrogen pressure in a tank [4],[6].

The described above tank failure mechanism in a fire implies that a tank with varying wall thickness will rupture when it will lose load-bearing ability in a location where the wall is the thinnest. The dome area is usually the thinnest compared to the cylindrical (sidewall) area. The wall thickness non-uniformity issue in the state-of-the-art designs of composite hydrogen tanks was raised previously. Composite-overwrapped tanks are manufactured implementing the filament winding process which includes the layup of helical and hoop layers in cylindrical/sidewall region and usually only helical layers in the dome region. The thickest region of the tank wall is the sidewall because of containing the hoop layers additionally to helical layers. The thinnest regions are usually the domes and they may be especially thin midways between the cylindrical part end and the boss neck. But, this mostly depends on the tank manufacturer and the design. These thinnest regions are sufficient to provide mechanical strength to the tank up to $P_{b.min.}$, that it is designed for. However, the dome is critically vulnerable to a fire and the tank FRR will be defined by degradation and failure in the dome region rather than sidewall [5], [8]. Figure 2 schematically demonstrates the tank composite overwrap performance in a fire in different regions at the same moment.

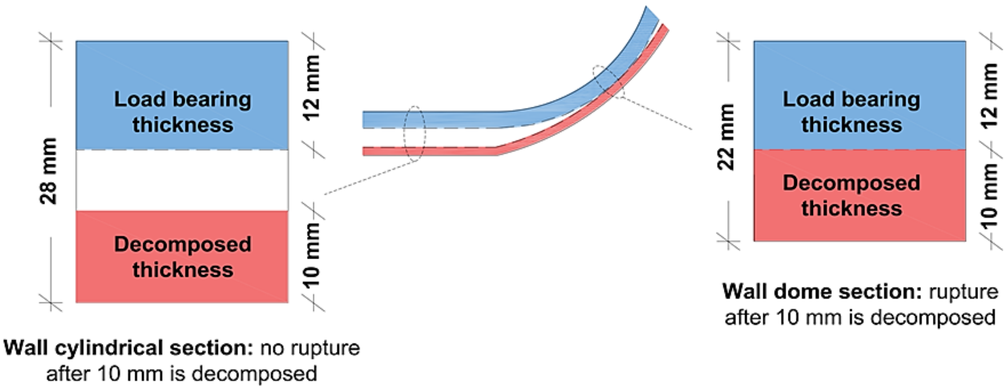

Figure 2. Wall thickness S_{CFRP} of the overwrap in the cylindrical/sidewall region (left) and in the dome region (right) and positions of load-bearing and decomposed fractions of wall thickness at the same time: no rupture conditions for the sidewall and rupture conditions for the dome [8].

In a fire, carbon fibres would be the last component of the composite to degrade thermally or can be not degraded at all, as noted in the experimental study [4]. In the worst case of tank rupture due to TPRD malfunction or localised fire when TPRD is not affected, the overall composite strength loss would be determined by the resin degradation, as per described above failure mechanism [5], [8]. The resin decomposition front progression is affected by the heat flux from the fire to the tank surface, resin decomposition temperature range, T_d, and the heat of decomposition, H_d, etc. Variations of these parameters affect the tank FRR.

Data on T_d of the resins found elsewhere shows that these usually range within 573-673 K (300-400°C). The relatively low decomposition temperatures can be 592 K, as per 10% of mass loss, as obtained by the thermogravimetric analysis [9]. In [10] it was stated that the first stage of decomposition (resin oxidative decomposition) occurs between 496-730 K. The decomposition temperatures published in [11], [12] are 623 K and 633 K respectively. Paper [13] provided data on T_d varying 569-639 K. Some applications have epoxy resins with T_d=713 K [14]. In paper [15] the T_d of the epoxy resins in composites with polypropylene content were analysed; T_d varied 553-648 K. The work [16] provides T_d=647 K. In our study we shall investigate the effect of resin T_d on the tank FRR, using the values within the above-reviewed ranges of 554-683 K [17] and 643-653 K [13], [16].

The heat of decomposition, H_d, also varies depending on the source. For instance, study [18] provides H_d=3.50·10^5 J/kg. Another differential scanning calorimetry study [17] of CFRP in nitrogen atmosphere helped to "isolate" resin decomposition from carbon with two temperature peaks at 652 K and 810 K respectively. The first temperature peak agrees with most of the met in literature values of T_d, where the mass loss is the highest, and where we assume the mechanical strength of the composite is lost (due to the loss of fibres' bonding). The second peak agrees well with the mentioned in another study temperature (813 K) [19] when the resin is completely degraded. The cumulative for these two stages heat of decomposition is H_d=3.48·10^4 J/kg + 3.04·10^{4}J/kg=6.52·10^4 J/kg.

This study aims to investigate the effect of the state of charge (SoC), burst pressure ratio (BPR) and thermal properties of a resin in composite tank overwrap, i.e. H_d and T_d, on tank FRR. The issue of the tank wall thickness non-uniformity on FRR is addressed also. The study will be performed using the validated non-adiabatic blowdown in a fire model [5], [8].

2.0 THE MODEL AND PARAMETERS OF THE STUDIED TANKS

The non-adiabatic blowdown in a fire model, including the failure mechanism of tank rupture in a fire, is described in [5], [8]. Here, the model is applied to simulate the pressure dynamics inside the tank, temperature distribution inside the composite wall, liner, and hydrogen temperature during the fire. The heat flux to the tank q'' from the fire at a specific heat release rate HRR/A=1 MW/m^2 was extracted from 3D simulations of the tank in a fire. The heat flux as a function of time used in our simulations is: q''= (-11.81$\cdot$ ln (t) + 113.97)$\cdot 10^3$ [5]. Table 1 represents the properties of the investigated three tanks, including thermal decomposition temperature and heat of decomposition.

Table 1. Tank material properties.

Parameter	Value	References
HDPE liner		
S_{HDPE}, mm	5.27	[20]
λ, W/m/K	0.4@293 K, 0.2@423 K	[21]
c_p, J/kg/K	2000@293 K, 2600@423 K	[21]
ρ, kg/m3	940	[21]
CFRP structural layer		
S_{CFRP}, mm	22.26	[20]
λ, W/m/K	Correlation	[17]
c_p, J/kg/K	Correlation	[17]
ρ, kg/m3	1360	[23]
H_d, J/kg	6.52·10^4 *	[17]
	3.50·10^5	[18]
	7·10^5 **	-
T_d, K	554-683	[17]
	643-653	[13],[16]

Notes: * - Sum of two degradation stages H_d=3.48·10^4 J/kg + 3.04·10^{4}J/kg=6.52·10^4 J/kg [17]; ** - Hypothetical value two times larger than the value referenced in this table of 2 $\cdot$ 3.50·10^5 J/kg=7·10^5 J/kg (this is for demonstration purpose, i.e. how the FRR changes if the tank manufacturer chooses the resin with the higher H_d).

Table 2 shows the difference in parameters of the three tanks studied in this paper.

Table 2. Parameters of three 70 MPa tanks.

Parameters	Tank#1 [20],[24],[25]	Tank#2 [26]	Tank#3 [6]
V, L	36	62.4	244
P_{NWP}, MPa	70		
Burst pressure ratio	2.25**		
D_{ext}, mm *	325	437	530
L, mm	909	748	2154
S_{CFRP}, mm *	27.75	24.3	33.36 [5]**
S_{HDPE}, mm *	3.8	3	3 [5] **

Notes: * - Sidewall (cylindrical) part; ** - assumptions;

It is assumed that all composite overwraps are made of the same CFRP and the liners are the same HDPE in all tanks, to be consistent in comparison to the tests. The initial tank and hydrogen gas temperature are 293.15 K, giving 70 MPa calculated SoC=99% (it is 100% for hydrogen T=288.15 K at 70 MPa).

3.0 EFFECT OF TANK SOC ON FIRE-RESISTANCE RATING

Figure 3 shows the dynamics of inward propagation of the resin decomposition front and outward propagation of the load-bearing wall thickness fraction for three initial pressures, i.e. NWP=70 MPa and reduced initial pressures 24 MPa and 17.8 MPa, in a 36 L volume tank. The simulations show that for initial pressure 70 MPa the tank ruptures after 402 s in the fire (when the two propagating in direction to each other fronts do meet).

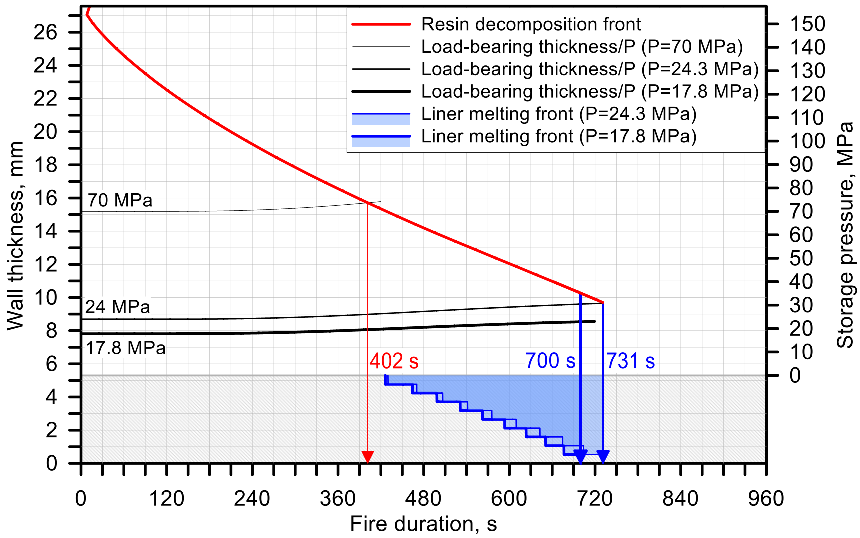

Figure 3. Performance of tank V=36 L, NWP=70 MPa in a fire with HRR/A=1 MW/m^2: rupture at initial pressure NWP=70 MPa (SoC=99%) and no rupture at initial pressures 24 MPa (SoC=43%) and 17.8 MPa (SoC=32.6%).

However, the decrease of pressure to 17.8 MPa for NWP=70 MPa, 36 L tank, the same as in the experiment [4], excludes tank rupture in the fire due to melting of the liner after 700 s in the fire that initiates hydrogen leakage through the wall. The tank's SoC in our simulation was 32.6% and calculated as follows. Hydrogen density at NWP=70 MPa and T=15ºC (288.15 K) is ρ=40.54 kg/m^3 (calculated by Abel-Noble equation for real gas). Hydrogen density at P=17.8 MPa and T=20ºC (293 K) is ρ=13.22 kg/m^3. Thus, the SoC for 17.8 MPa is SoC=[13.22 kg/m^3 / 40.54 kg/m^3]×100%=32.6%.

The simulated performance in the fire of the NWP=70 MPa tank with the initial pressure of 17.8 MPa resulting in no rupture but leakage, is the accurate reproduction of the result observed in fire tests with the same tanks at an initial pressure of 17.8 MPa [4]. Afterwards, in the simulation, we increase the pressure to the maximum upper bound value, above which there will be tank rupture. The initial pressure of 24 MPa (SoC=42.5%) was found to be "on the border" between rupture and leak and this is very close to the experimental value of 25 MPa [6] (only 4% difference), where the leak without burst was observed.

The performance of the 62.4 L tank at 70 MPa (rupture) and 30 MPa (no rupture) is shown in Figure 4.

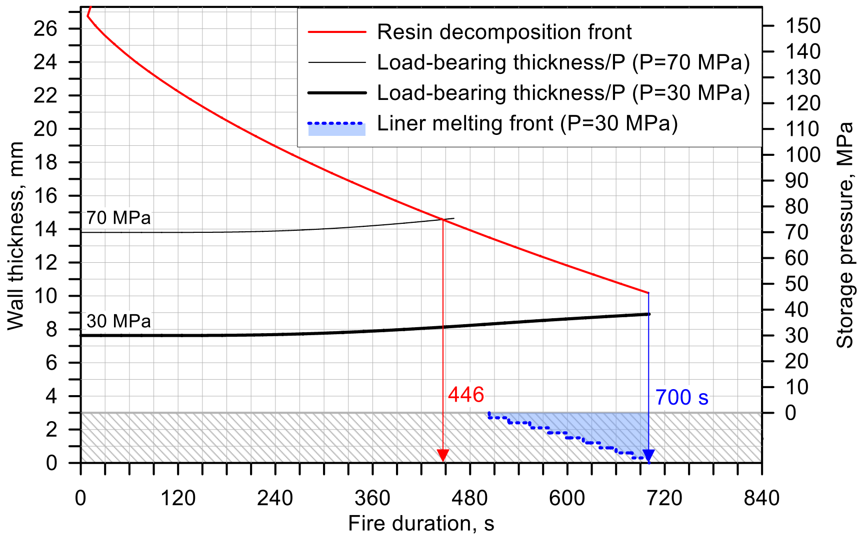

Figure 4. Performance of tank V=62.4 L, NWP=70 MPa in a fire with HRR/A=1 MW/m^2: rupture at initial pressure NWP=70 MPa and no rupture at initial pressure 30 MPa.

Figure 4 demonstrates that the 62.4 L, NWP=70 MPa tank will not rupture in the fire if hydrogen pressure inside the tank is 30 MPa (SoC=51%). This is thought due to the increased wall thickness for the tank of bigger volume, and the thinner liner, making its melting faster.

The performance of the 244 L, NWP=70 MPa tank at pressure 70 MPa (rupture) and 32 MPa (no rupture) is shown in Figure 5.

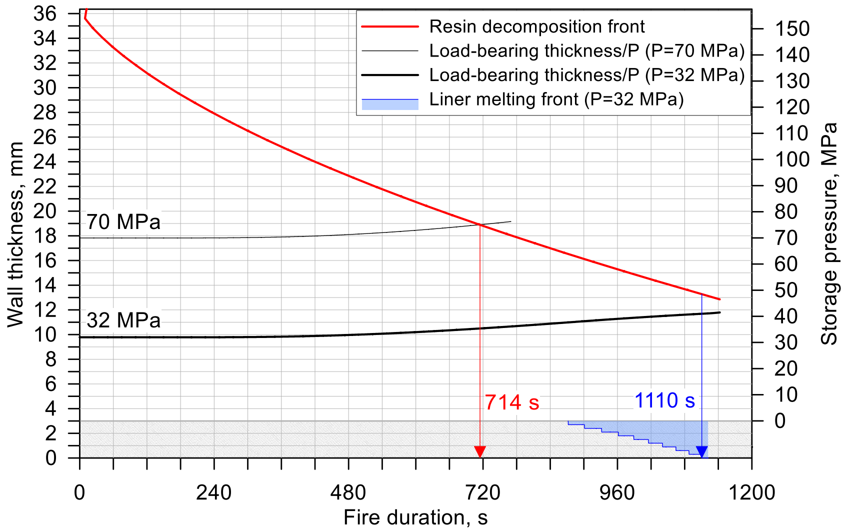

Figure 5. Performance of tank V=244 L, NWP=70 MPa in a fire with HRR/A=1 MW/m^2: rupture at initial pressure NWP=70 MPa and no rupture at initial pressure 32 MPa.

Figure 5 shows a similar to 62.4 L tank trend, but the initial hydrogen pressure sufficient for leak and rupture prevention is slightly higher, i.e. 32 MPa (SoC=54%), as the composite is thicker in 244 L tank.

4.0 EFFECT OF TANK WALL THICKNESS NON-UNIFORMITY ON THE FRR

Assuming both the dome and the sidewall of the tank are subject to a fire, Figure 6 shows the performance of both these parts in a fire for 36 L, NWP=70 MPa tank causing a rupture and lowered pressure preventing rupture by causing hydrogen leak.

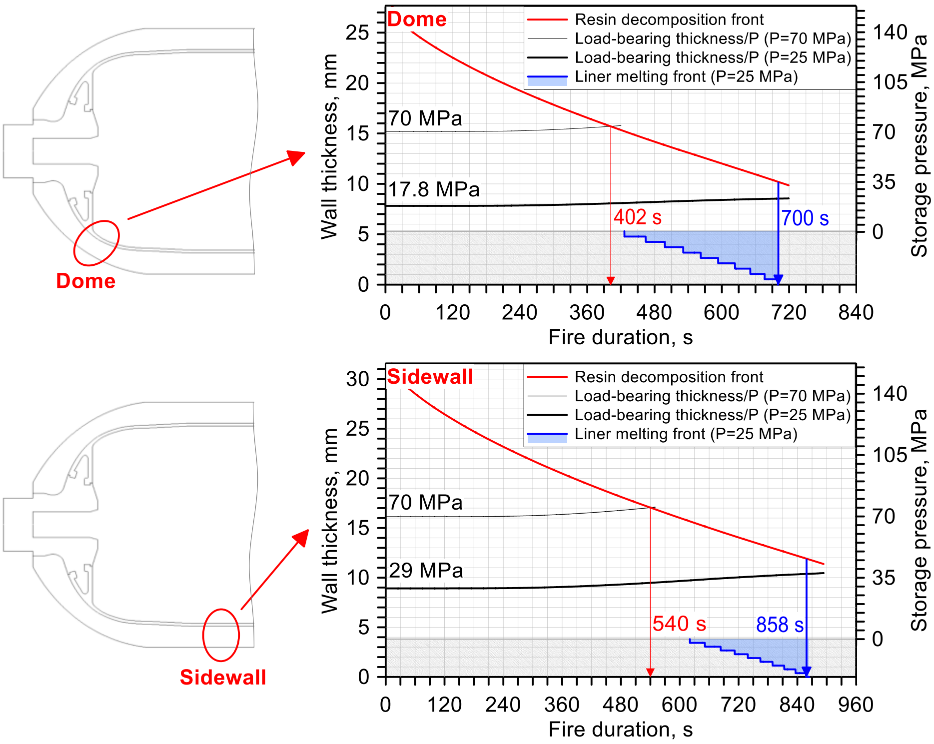

Figure 6. Performance of tank V=36 L, NWP=70 MPa in a fire with HRR/A=1 MW/m^2: effect of thinner wall thickness in the dome (top) and thicker sidewall (bottom) for two initial pressures, i.e. NWP=70 MPa and the pressure below which the liner melts and the tank rupture is excluded (17.8 MPa and 29 MPa respectively).

In the considered example of 36 L, NWP=70 MPa tank the dome part has liner thickness 5.27 mm and CFRP thickness 22.26 mm while the sidewall has 3.81 mm and 27.75 mm for liner and CFRP respectively. The thickened liner in the dome region is probably the manufacturer's technical necessity due to the liner and boss connection.

Figure 6 demonstrates that, as expected, at NWP=70 MPa the increase of composite wall thickness by 20% from 22.26 mm (dome) to 27.75 mm (sidewall) results in an increase of FRR by 34%, i.e. from 402 s (6 min 42 s) to 540 s (9 min). The initial pressure that prevents rupture is higher for the thicker sidewall. The liner melts in the sidewall at an initial pressure of 29 MPa (SoC=50%) (Figure 6, bottom), while for the dome region it is only 17.8 MPa (SoC=32.6%) (Figure 6, top). In the engulfing fire, the tank would rupture at the dome area after 402 s while the sidewall still can bear the load. This is an apparent disadvantage in the current design of composite storage tanks that must be addressed by tank manufacturers and OEMs.

5.0 EFFECT OF THE BURST PRESSURE RATIO ON THE FRR

In this section, the effect of BPR on FRR for NWP=70 MPa tanks will be assessed. The minimum regulated BPR for CFRP is currently 2.25. The increase of BPR by a manufacturer does not violate the regulations. The described above 36 L tank with the defined thickness at the dome and sidewall areas is used in our calculations in the assumption that composite fibres strength is different. The difference in fibres strength allows having the same wall thickness but different BPR which is the ratio of burst pressure to NWP. It was underlined above that the dome is the most vulnerable to fire. Thus, considering the dome part, the calculation results of the tank performance at several BPRs: 2.00, 2.25, 2.5 and even 3 are given below. The increase of the BPR from 2.00 to say 2.5 means that the burst pressure also increases from 2*70=140 MPa to 2.5*70=175 MPa. We also expect that the higher BPR will decrease $S_{load\ b.}$ and hence increase “load+” and thus the tank FRR. Figure 7 shows the effect of BPR for 36 L, NWP=70 MPa tank of the same geometry but different strength fibres on its FRR.

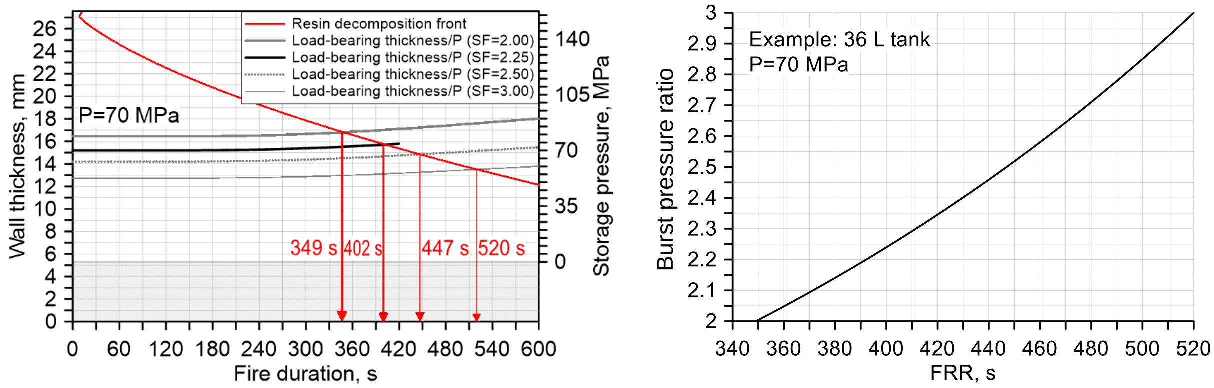

Figure 7. Performance of tank V=36 L, NPW=70 MPa made of different strength fibres in a fire with HRR/A=1 MW/m^2. Left: effect of BPR on FRR (dynamics of $S_{load\ b.}$ and resin decomposition front. Right: dependence between FRR and BPR in the range BPR=2-3.

Figure 7 demonstrates an increase in the tank FRR with the increase of its BPR. For instance, the decrease of regulated BPR from 2.25 to 2 shortens FRR from 402 (6 min 42 s) s to 349 s (5 min 49 s), i.e. by 13%. The increase of BPR from 2.25 to 2.5 increases the FRR to 447 s (7 min 27 s), i.e. by 11%. The highest FRR increase by 29% to 520 s (8 min 40 s) is for the BPR increase from 2.25 to 3.

6.0 EFFECT OF RESIN THERMAL PROPERTIES, T_d AND H_d, ON THE FRR

This section studies how the parameters of resin in composite, such as H_d and T_d, affect the resin decomposition front propagation and hence the tank FRR. Firstly, we shall fix H_d=3.5·10^5 J/kg and change the decomposition temperature ranges to see the effect of T_d on the FRR. T_d range as 554-683 K (as in all previous simulations) and a higher one of 643-653 K (initial T_d increased by 89 K), as per references in Table 1, will be used in the calculations. The FRR results for 36 L at NWP=70 MPa and lower pressures sufficient to make liner melt and prevent tank rupture are shown in Figure 8.

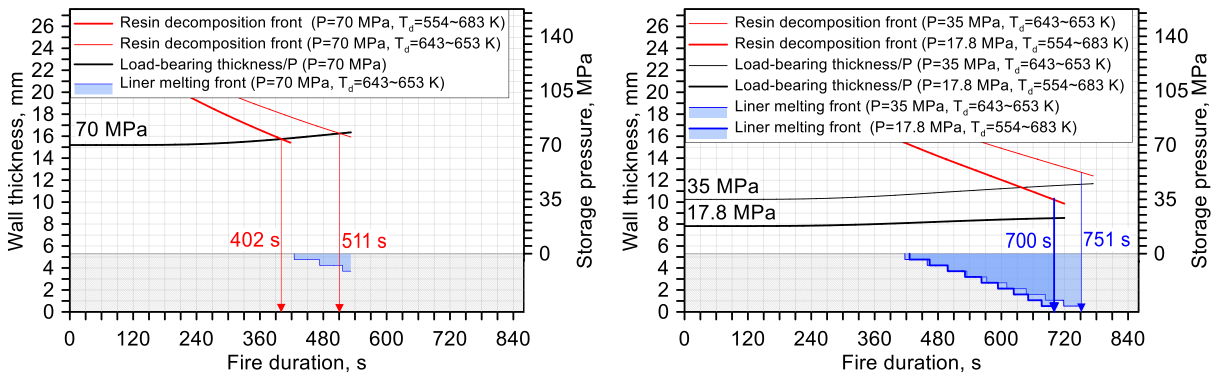

Figure 8. Performance of tank V=36 L, NWP=70 MPa in a fire with HRR/A=1 MW/m^2: effect of resin T_d on the tank FRR at fixed H_d=3.5·10^5 J/kg. Left: effect of T_d on FRR. Right: effect of T_d on the upper-pressure limit that excludes tank rupture and time to leak.

Figure 8 (left) demonstrates that higher T_d (by 16%, as compared in Kelvin) increases the tank FRR from 402 s (6 min 42 s) to 511 s (8 min 31 s), i.e. by 27%. It also allows preventing tank rupture by melting liner at higher hydrogen pressure inside the tank of 35 MPa (SoC=58%) instead of 17.8 MPa (SoC=32.6%) as shown in Figure 8 (right).

Figure 9 shows the effect of three different H_d on tank FRR at the fixed T_d range 554-683 K.

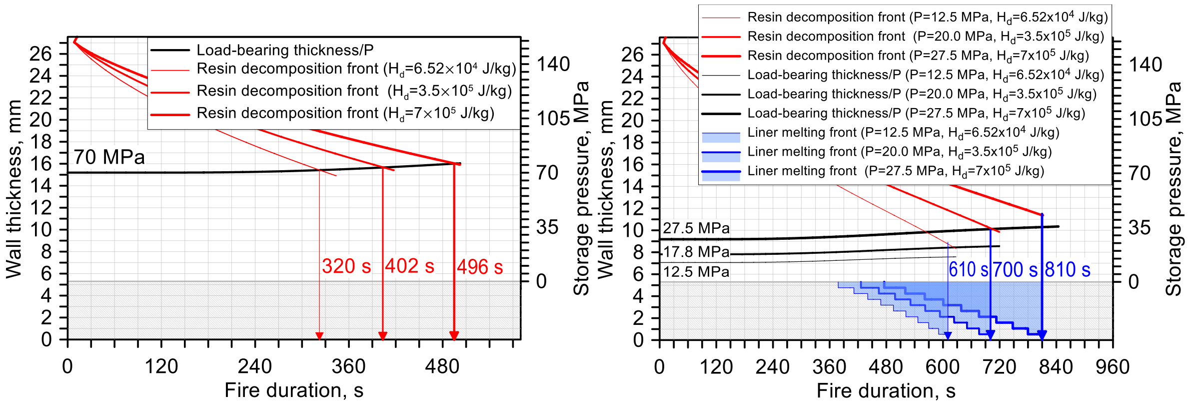

Figure 9. Performance of tank V=36 L, NWP=70 MPa in a fire with HRR/A=1 MW/m^2: effect of different resin H_d on the tank FRR at fixed T_d range 554-683 K .

The increase of the resin H_d increases the tank FRR (Figure 9, left). For instance, the previously used $3.5 \cdot 10^5$ J/kg compared to hypothetical value $7 \cdot 10^5$ J/kg (100% increase) rises the tank FRR from 402 s to 496 s (8 min 16 s), i.e. by 23%. In this respect, we see that doubling of resin H_d gives a relatively small FRR increase. It can be concluded that the effect of T_d is stronger compared to that of H_d resulting in almost equivalent increase of FRR with T_d (27% and 16% respectively). Figure 9 (right) shows that the higher is the resin H_d, the higher is the upper limit of pressure inside the tank which prevents tank rupture due to the liner melting, i.e. 12.5 MPa (SoC=24%), 17.8 MPa (SoC=32.6%) and 27.5 MPa (SoC=48%).

CONCLUSIONS

The effect of 70 MPa Type IV tank SoC on the FRR is studied using a previously validated model of non-adiabatic tank blowdown in fire conditions including the original composite tank failure in a fire mechanism. The experimentally observed phenomenon of tank leaking instead of rupture in a fire at initial pressures below about NWP/3 is accurately reproduced in the simulations and underlying physics is discussed. The effect of tank wall non-uniformity on the reduction of the tank FRR is studied, and it is concluded that tank manufacturers must address this issue to provide a higher level of life safety and property protection through the increased FRR. The effect of composite properties such as the resin heat of decomposition, H_d, and range of decomposition temperatures, T_d, as well as the burst pressure ratio (BPR) on the tank FRR is investigated and understood. The FRR increases with the increase of T_d and H_d, yet the effect of T_d is more pronounced. These findings define the *originality* of this work.

The *significance* of the study is in the closure of knowledge gaps in understanding a tank performance in a fire at different SoC, the effect of wall non-uniformity, burst pressure ratio and thermal parameters of the composite on the FRR. The tanks of NWP=70 MPa and volumes 36 L, 62.4 L and 244 L do not rupture in a fire at SoC=32.6%, i.e. hydrogen pressure of 17.8 MPa (with the possible rupture avoidance at pressures up to 24 MPa, i.e. SoC=43%), SoC=51% (30 MPa) and SoC=54% (32 MPa) respectively. The wall thicknesses non-uniformity of the selected industrial 36 L tank demonstrated the difference in FRR of 34%. The wall BPR was found to increase the tank FRR by 23% for BPR increase from 2.25 to 3. It was shown that the increase of resin T_d has a stronger effect on the FRR increase than H_d. The avoidance of a catastrophic tank rupture in a fire at a decreased

SoC due to melted liner and hydrogen release is only possible for Type IV tanks, and not for Type III tanks, where the liner is metallic. This is a safety advantage of Type IV tanks.

The *rigour* of this study is in the reproduction of the experimentally observed phenomenon of leaking of tanks at hydrogen pressures below about NWP/3 including due to the use of referenced thermal parameters in simulations. The numerical tests performed for the industrial 36 L, NWP=70 MPa tank and decreased initial pressure down to 24 MPa (and below) was found sufficient to prevent rupture due to the liner melting and follow-up leakage of hydrogen through the tank wall. This pressure is in line with experimentally registered pressure 25 MPa [6] (4% difference) when the tank leakage instead of rupture was observed. Further pressure decrease to 17.8 MPa, matching with equivalent experimental pressure [4], also provided the rupture avoidance due to liner melting, as observed in the corresponding experiment [4]. The rigour of the work is also underpinned by the range of studied parameters that affect the FRR. These include the SoC below 100% including the limits of SoC below which the tanks leak in the fire instead of rupture; the wide range of tanks' volumes, i.e. 36 L, 62.4 L and 244 L, etc.

ACKNOWLEDGEMENTS

The authors are grateful to Fuel Cells and Hydrogen 2 Joint Undertaking (FCH2 JU) for funding this research through the SH2APED project. The SH2APED project has received funding from the FCH2 JU under grant agreement No.101007182. This Joint Undertaking receives support from the European Union's Horizon 2020 research and innovation programme, Hydrogen Europe and Hydrogen Europe Research.

REFERENCES

1. Dadashzadeh, M., Kashkarov, S., Makarov, D., and Molkov, V., Risk assessment methodology for onboard hydrogen storage, *Int. J. Hydrog. Energy*, **43**, no. 12, 2018, pp. 6462–6475.
2. SAE J2601, SURFACE VEHICLE STANDARD, (R) Fueling Protocols for Light Duty Gaseous Hydrogen Surface Vehicles, 2016.
3. United Nations Economic Commission for Europe, Global Registry. Addendum 13: Global technical regulation No. 13. Global technical regulation on hydrogen and fuel cell vehicles, UNECE, 2013.
4. Ruban, S. *et al.*, Fire risk on high-pressure full composite cylinders for automotive applications, *Int. J. Hydrog. Energy*, **37**, no. 22, 2012, pp. 17630–17638.
5. Molkov, V., Dadashzadeh, M., Kashkarov, S., and Makarov, D., Performance of hydrogen storage tank with TPRD in an engulfing fire, *Int. J. Hydrog. Energy*, 2021 (submitted for publication).
6. Blanc-Vannet, P. *et al.*, Fire tests carried out in FCH JU Firecomp project, recommendations and application to safety of gas storage systems, *Int. J. Hydrog. Energy*, no.17, 2019, pp. 9100–9109.
7. Commission Regulation, No 406/2010 implementing Regulation (EC) No 79/2009 of the Parliament and of the Council on type-approval of hydrogen-powered vehicles, *Off. J. Eur. Union*, 2010.
8. Dadashzadeh, M., Makarov, D., Kashkarov, S., and Molkov, V., Non-adiabatic under-expanded jet theory for blowdown and fire resistance rating of hydrogen tank, Proceedings of the International Conference on Hydrogen Safety, 2019, Adelaide, Australia.
9. Liu, W., Varley, R. J., and Simon, G. P., Understanding the decomposition and fire performance processes in phosphorus and nanomodified high performance epoxy resins and composites, **48**, 2007, pp. 2345–2354.
10. Branca, C., Di Blasi, C., Galgano, A., and Milella, E., Thermal and kinetic characterization of a toughened epoxy resin reinforced with carbon fibers, **517**, 2011, pp. 53–62.
11. Merino-Pérez, J. L., Hodzic, A., Merson, E., and Ayvar-Soberanis, S., On the temperatures developed in CFRP drilling using uncoated WC-Co tools Part II: Nanomechanical study of thermally aged CFRP composites, **123**, 2015, pp. 30–34, 2015.
12. Pan, C. T. and Hocheng, H., Evaluation of anisotropic thermal conductivity for unidirectional FRP in laser machining, **32**, 2001, pp. 1657–1667.

13. Régnier, N. and Fontaine, S., Determination of the thermal degradation kinetic parameters of carbon fibre reinforced epoxy using TG, **64**, 2001, pp. 789–799.
14. PerkinElmer Inc, Characterization of Polymers Using TGA. http://www.perkinelmer.com/CMSResources/Images/44-132088APP_CharacterizationofPolymersUsingTGA.pdf (accessed Apr. 24, 2015).
15. Niranjana Prabhu, T., Hemalatha, Y. J., Harish, V., Prashantha, K., and Iyengar, P., Thermal Degradation of Epoxy Resin Reinforced with Polypropylene Fibers, *Wiley InterScience*, 2006. www.interscience.wiley.com (accessed Apr. 24, 2015).
16. Chiang, C.L., Chang, R.C., and Chiu, Y.C., Thermal stability and degradation kinetics of novel organic/inorganic epoxy hybrid containing nitrogen/silicon/phosphorus by sol–gel method, **453**, 2007, pp. 97–104.
17. Welch, S., Hadden, R., Hidalgo-Medina, J., and Pironi, P., Thermal properties and thermal modelling of composite materials exposed to fires, 2017, University of Bath.
18. J Hu, J., Chen, J., Sundararaman, S., Chandrashekhara, K., and Chernikoff, W., Analysis of composite hydrogen storage cylinders subjected to localized flame impingements, *Int. J. Hydrog. Energy*, **33**, 2008, pp. 2738–2746.
19. Yatim, N. M., Shamsudin, Z., Shaaban, A., Sani, N. A., Jumaidin, R., and Shariff, E. A., Thermal analysis of carbon fibre reinforced polymer decomposition, *Mater. Res. Express*, **7**, no. 1, 2020, p. 015615.
20. Heggem, P., Private communication, 2013.
21. Kashkarov, S., Makarov, D., and Molkov, V., Model of 3D conjugate heat transfer and mechanism of compressed gas storage failure in a fire, presented at the International Conference on Hydrogen Safety, 2017, Hamburg, Germany.
22. ‘NIST. Isothermal properties for hydrogen’, 2017. http://webbook.nist.gov/cgi/inchi?ID=C1333740&Mask=1#Thermo-Gas (accessed 17.03.2021).
23. Monde, M. and Kosaka, M., ‘Understanding of thermal characteristics of fueling hydrogen high pressure tanks and governing parameters’, *SAE Int. J. Alt. Power.*, 2013, pp. 61–67.
24. Kashkarov, S., Makarov, D., and Molkov, V., Effect of a heat release rate on reproducibility of fire test for hydrogen storage cylinders, *Int. J. Hydrog. Energy*, **43**, no. 21, 2018, pp. 10185–10192.
25. Saldi, Z. and Wen, J. X., Modeling thermal response of polymer composite hydrogen cylinders subjected to external fires, Proceedings of the International Conference on Hydrogen Safety, 2015, Yokohama, Japan.
26. Mattelaer, V., Private communication, 2018.